Effect of an intense radiation field on the discrete and continuum spectra of atomic hydrogen

Y. Gontier and M. Trahin
Institut de Recherche Fondamentale, Service de Physique des Atomes et des Surfaces, Centre d'Etudes Nucléaires de Saclay, 91191 Gif-sur-Yvette CEDEX, France
(Received 12 December 1988)

Second-order and fourth-order intensity-dependent corrections to the energy levels of the hydrogen atom are calculated. By comparing the results obtained for these two orders and for various values of the principal quantum number, it is seen that, at a given intensity, the second-order correction becomes more and more questionable as one approaches the ionization limit. It is shown how the divergences, which appear in calculating the matrix elements of the shift operator in a discrete basis of continuum functions, can be avoided by performing the computation in the velocity gauge. The relevant second-order numerical results indicate serious modifications of the continuum spectrum. Intrinsic limitations of the second-order calculations are discussed.

I. INTRODUCTION

Theories involving the resolvent operator (resonant ionization, above-threshold ionization) require the knowledge of matrix elements of an operator $R(z)$ (Refs. 1–11) which must be evaluated over the complete set of atomic states. The nondiagonal matrix elements provide the probability amplitude for the transitions while the diagonal ones are related to the shift and the width of the atomic levels. Two situations arise according to whether the levels lie in the discrete spectrum or in the continuum of the atom. The case of discrete levels has been discussed at length in the literature.[12–14] In most cases only the lowest-order nonvanishing term $R^{(2)}(E)$ of the perturbation expansion of $R(z)$ is taken into account. This approximation has proved to be largely sufficient to expound experiments on resonantly enhanced multiphoton ionization of Cs (Ref. 13) and atomic hydrogen.[14] Yet it leads to theoretical predictions in excellent agreement with the measurements of the shift of Rydberg energy levels.[15,16] This agreement is due to the fact that the above-mentioned experiments were done at moderate intensity ($<10^{10}$ W/cm^2). Recently, two experiments[17,18] on multiphoton ionization of Xe have been done at high intensity (10^{13}–10^{14}W/cm^2). The fine structures observed on the electron spectrum are interpreted within a model where the shifts of the discrete levels play the dominant role. In these experiments the intensity is so large that one may ask to what extent the values of the shifts calculated from second-order perturbation theory are reliable.

In Sec. II we briefly recall the basic expressions involving $R(z)$. In Sec. III we report numerical values concerning $R^{(2)}_{n,n}$. The calculations have been done in the length and in the velocity gauges for states from $n=1$ to 40 (n being the principal quantum number). The comparison between the results obtained separately in the two gauges shows the role played by the quadratic A^2 term of the interaction Hamiltonian. It produces a shift of the whole spectrum of the atom and thus cannot give rise to physical effects in processes whose behavior is governed by energy-level differences. The values of the fourth-order contribution to $R^{\mathrm{diag}}(E)$ are presented in Sec. IV for states from $n=1$ to 10 in the case of circularly polarized light. Except for some values concerning the hydrogen atom in the ground state,[12,19–21] these results seem to be quite new. They are very useful to test the convergence of the perturbation expansion of $R^{\mathrm{diag}}(E)$. By comparing second-order and fourth-order terms, we show that this series diverges rapidly when the intensity and/or the principal quantum number increase. Next, the corrections to the ground-state energy of hydrogen are discussed by investigating the effects of the first three terms of the perturbation expansion in the case of linearly polarized light. Our results are compared to those obtained from "nonperturbative" theories.[21,22]

The last part of the paper is devoted to problems arising from the construction of a matrix representation of the shift operator in the continuum spectrum. The investigations of processes such as above-threshold ionization (ATI), require the evaluation of integrals over continuum states. This is done by numerical quadratures which are generated by the discretization of the second-order operator $R^{(2)}(E)$ in a finite basis of continuum wave functions $|\alpha,E\rangle$. Although the complex matrix eigenvalues of $R^{(2)}(E)$ cannot be measured directly, we generalize for a practical purpose the concept of level shifts and level widths to continuum states.[23]

The electrons generated in the αth continuum could take any one of the p_α discrete energy values used to define the basis set. From the formulation of the ATI process given in Sec. II we shall see that the probability density to find an electron in the αth continuum, at the energy E, is a strongly dependent function of $R^{(2)}_{\alpha E\alpha E}$. In Sec. V, the matrix elements of $R^{\mathrm{diag}}(E)$ are written in terms of the length operator. The divergences which do not appear explicitly in the usual expression of the shift are localized. They come from the energy degeneracy occurring in the matrix element $\langle \alpha E|\boldsymbol{\varepsilon}\cdot\mathbf{r}|\alpha' E'\rangle$, when

$E=E'$. Such a difficulty which is typical of the multiphoton theory does not seem to have been solved up to now.[20] In order to put the continuum-continuum second-order matrix elements into a fully tractable form, we present an original calculation scheme which allows us to evaluate exactly the integrals encountered in the problem. In Sec. VI, the complex values of the second-order shift operator are given as functions of the energy and the orbital quantum number at $\Lambda=1060$ nm. The intrinsic limitations of the lowest-order perturbation theory are discussed in Sec. VII.

II. SHIFT OPERATOR

The matrix elements of the operator $R(z)$ mentioned in the Introduction are usually computed over a few particular states of H_0, the free Hamiltonian of the system atom plus field. In the subspace ϵ spanned by these particular states, the expression of the resolvent operator for the total Hamiltonian H_0+V (V represents the interaction), which reads

$$G(z)=\frac{1}{z-H_0-V} , \tag{2.1}$$

transforms into

$$\tilde{G}(z)=\frac{1}{z-H_0-\tilde{R}(z)} , \tag{2.2}$$

where

$$\tilde{G}(z)=PG(z)P , \tag{2.3a}$$

$$\tilde{R}(z)=PR(z)P . \tag{2.3b}$$

The shift operator $R(z)$ can be expanded in powers of V as

$$R(z)=V+V\frac{Q}{z-H_0}V+V\frac{Q}{z-H_0}V\frac{Q}{z-H_0}V+\cdots . \tag{2.4}$$

The operators P and Q are the projectors onto and outside the subspace ϵ, respectively. From Eq. (2.2) $\tilde{G}(z)$ is the resolvent operator of the Hamiltonian

$$\tilde{H}(z)=H_0+\tilde{R}(z) . \tag{2.5}$$

As a result of the resummation of the series given by Eq. (2.4), one finds that the diagonal and the nondiagonal parts of $R(z)$ are[9]

$$R^{(D)}(z)=[V^+\bar{G}^0(z)\bar{V}^-\bar{G}^-(z)+V^-\bar{G}^0(z)\bar{V}^+\bar{G}^+(z)](z-H_0) , \tag{2.6a}$$

$$R^{(ND)}(z)=\{V^\pm\bar{G}^0(z)[\bar{V}^\mp\bar{G}^\mp(z)]^{N+1}+V^\mp\bar{G}^0(z)[\bar{V}^\mp\bar{G}^\mp(z)]^{N-1}\}(z-H_0) , \tag{2.6b}$$

respectively. In Eq. (2.6b), the upper (lower) sign is to be taken for the net absorption (emission) of N photons, while $\bar{G}^0(z)$ and $\bar{G}^\pm(z)$ are continued fractions of $\bar{V}^\pm=QV^\pm$ (V^+ and V^- are the photon emission and the photon absorption operators, respectively). One has[9]

$$\bar{G}^\pm(z)=\frac{1}{z-H_0-\bar{V}^\pm\bar{G}^\pm(z)\bar{V}^\mp} , \tag{2.7a}$$

$$\bar{G}^0(z)=\frac{1}{z-H_0-\bar{V}^+\bar{G}^+(z)\bar{V}^--\bar{V}^-\bar{G}^-(z)\bar{V}^+} . \tag{2.7b}$$

As an example, let the subspace ϵ be a two-dimensional space spanned by the ground state $|0\rangle$ and the continuum $|\alpha E\rangle$. We recall that the transition amplitude corresponding to the transition $|0\rangle\rightarrow|\alpha E\rangle$, which involves the absorption of $N+S$ photons of energy ω (i.e., above-threshold ionization with absorption of S extra photons in the continuum), is given by

$$U_{\alpha E,0}(t)=\frac{1}{2\pi i}\oint e^{-izt}G_{\alpha E,0}(z)dz , \tag{2.8}$$

where

$$G_{\alpha E,0}(z)=\frac{R_{\alpha E,0}(z)}{[z-E+(N+S)\omega-R_{\alpha E,\alpha E}(z)][z-E_0-R_{0,0}(z)]-R_{\alpha E,0}(z)R_{0,\alpha E}(z)} . \tag{2.9}$$

Equation (2.9) shows that the diagonal matrix elements of $R(z)$ are not exactly the level shifts. The true level shifts are obtained from the poles of the expression displayed on the right-hand side of this equation, i.e., the two values $z^\pm$ of z for which the denominator vanishes. In this calculation scheme, the states contributing to the shift are mixed through matrix algebra so that the computation involves complicated couplings among atomic states which make necessary a numerical analysis.

The transition amplitude derived from Eqs. (2.8) and (2.9) becomes

$$U_{\alpha E,0}(t)=\frac{1}{z^+-z^-}[R_{\alpha E,0}(z^+)e^{-iz^+t}-R_{\alpha E,0}(z^-)e^{-iz^-t}] . \tag{2.10}$$

By neglecting the term $(R_{\alpha E,0}R_{0,\alpha E})$ in Eq. (2.9), one finds that the approximate expressions for z^+ and z^- are

$$z^+\simeq E-(N+S)\omega+\mathrm{Re}[R_{\alpha E,\alpha E}(E-(N+S)\omega)]-i\,\mathrm{Im}[R_{\alpha E,\alpha E}(E-(N+S)\omega)] , \tag{2.11a}$$

$$z^-\simeq E_0+\mathrm{Re}[R_{0,0}(E_0)]-i\,\mathrm{Im}[R_{0,0}(E_0)] . \tag{2.11b}$$

Finally, the probability of finding an electron at time t in the αth continuum is

$$P_\alpha(t)=\int_0^\infty|U_{\alpha E,0}(t)|^2dE . \tag{2.12}$$

This probability is calculated in a finite basis of discrete and continuum eigenfunctions of the Hamiltonian H_0. In Eq. (2.12) the integral over the αth-continuum spectrum

is evaluated by performing the quadrature generated by the discretization of the operator $R(E)$ in a finite set of p_α continuum wave functions $|\alpha E\rangle$. The basis functions provide a matrix representation of $R(E)$ whose the diagonal elements may be interpreted as the shift and the width associated with the continuum state $|\alpha E\rangle$. Equations (2.10) and (2.11) outline the central role played by the diagonal matrix elements of $R(z)$ when the time dependence and the magnitude of the transition probabilities are investigated.

III. SECOND-ORDER ENERGY SHIFT IN THE DISCRETE SPECTRUM

In the length gauge the total Hamiltonian operator is

$$H=\frac{\mathbf{P}^2}{2}-\frac{1}{r}-\mathbf{r}\cdot\mathbf{E}\ . \tag{3.1}$$

The second-order energy shift in atomic units is given by

$$R^{(2)}_{n,n}=\frac{I}{I_0}\sum_j{}'\left[\frac{D^*_{n,j}D_{j,n}}{E_n-E_j+\omega}+\frac{D_{n,j}D^*_{j,n}}{E_n-E_j-\omega}\right], \tag{3.2}$$

where

$$D_{n,j}=\langle n|\boldsymbol{\varepsilon}\cdot\mathbf{r}|j\rangle\ , \tag{3.3}$$

and $I_0=1.4038\times10^{17}$ W/cm^2. The prime on the summation indicates that the sum runs over the complete (discrete plus continuum) spectrum of H_0.

Strictly speaking, the true level shifts of discrete states are obtained by averaging $R^{(2)}_{n,n}$, as given by Eq. (3.2), over the degenerate states. Nevertheless, recent works show that this average provides corrections less than 2%.[12] Thus $R^{(2)}_{n,n}$ will be considered as being the level shift throughout this paper.

The diagrams contributing to second-order processes are illustrated in Fig. 1(a) in the energy scale. The photon energy and the atomic levels have been chosen in such a way that the intermediate virtual states lie above the ionization limit. The energy $E_n+\omega$ is thus positive and the shift is complex. This can be seen by writing explicitly the summations running over the discrete spectrum and the continuum. Equation (3.2) reads as

$$R^{(2)}_{n,n}=\frac{I}{I_0}\left[\sum_j\left[\frac{D^*_{n,j}D_{j,n}}{E_n-E_j+\omega}+\frac{D_{n,j}D^*_{j,n}}{E_n-E_j-\omega}\right]+\int_0^\infty dE\left[\frac{D^*_{n,\alpha E}D_{\alpha E,n}}{E_n-E+\omega}+\frac{D_{n,\alpha E}D^*_{\alpha E,n}}{E_n-E-\omega}\right]\right], \tag{3.4}$$

where only the third term on the right-hand side of the equation contains a pole around $E=E_n+\omega$. The corresponding integral can be calculated in the usual way by using the well-known identity

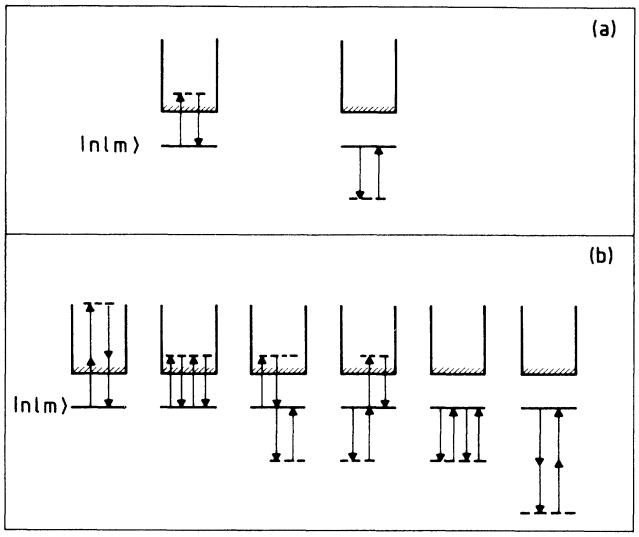

FIG. 1. Diagrams representing (a) the second-order and (b) the fourth-order corrections to the energy of any discrete ($|nlm\rangle$) or continuum state ($|Elm\rangle$).

$$\int_0^\infty dE\frac{D^*_{n,\alpha E}D_{\alpha E,n}}{E_n-E+\omega}\rightarrow \mathrm{P}\int_0^\infty dE\frac{D^*_{n,\alpha E}D_{\alpha E,n}}{E_n-E+\omega}-i\pi(D^*_{n,\alpha E}D_{\alpha E,n})_{E=E_n+\omega}\ , \tag{3.5}$$

where P means the Cauchy principal value of the integral. The imaginary term in Eq. (3.5) provides the width of the level (nlm), while the real part together with the remaining (real) terms in Eq. (3.4) are the contributions to the shift of the level.

The matrix elements of the second-order shift operator can also be expressed within the velocity gauge where the Hamiltonian reads

$$H=\frac{\mathbf{P}^2}{2}-\frac{1}{r}-\alpha\,\mathbf{A}\cdot\mathbf{P}+\frac{\alpha^2}{2}\mathbf{A}^2\ , \tag{3.6}$$

α being the fine-structure constant.

In this case the expression of $R_{n,n}$ becomes

$$R^{(2)}_{n,n}=\frac{I}{I_0\omega^2}\left[1+\sum_j{}'\left[\frac{(\boldsymbol{\varepsilon}^*\cdot\mathbf{P})_{nj}(\boldsymbol{\varepsilon}\cdot\mathbf{P})_{jn}}{E_n-E_j+\omega}+\frac{(\boldsymbol{\varepsilon}\cdot\mathbf{P})_{nj}(\boldsymbol{\varepsilon}^*\cdot\mathbf{P})_{jn}}{E_n-E_j-\omega}\right]\right]. \tag{3.7}$$

Obviously Eqs. (3.4) and (3.7) are completely equivalent. In addition, one can easily find the connection between the two gauges. By using the formula $(\boldsymbol{\varepsilon}\cdot\mathbf{P})_{ij}=iE_{ij}(\boldsymbol{\varepsilon}\cdot\mathbf{r})_{ij}$ together with the commutation relation $\varepsilon_i\varepsilon_f\delta_{if}=i[(\mathbf{P}\cdot\boldsymbol{\varepsilon}_i),(\mathbf{r}\cdot\boldsymbol{\varepsilon}_f)]_{fi}$, one obtains

$$\sum_j{}'\frac{(\boldsymbol{\varepsilon}^*\cdot\mathbf{r})_{nj}(\boldsymbol{\varepsilon}\cdot\mathbf{r})_{jn}}{E_{nj}+\omega}=\frac{1}{\omega^2}\sum_j{}'\left[\frac{(\boldsymbol{\varepsilon}^*\cdot\mathbf{P})_{nj}(\boldsymbol{\varepsilon}\cdot\mathbf{P})_{jn}}{E_{nj}+\omega}+(E_{jn}+\omega)(\boldsymbol{\varepsilon}^*\cdot\mathbf{r})_{nj}(\boldsymbol{\varepsilon}\cdot\mathbf{r})_{jn}\right], \tag{3.8a}$$

$$\sum_j{}' \frac{(\boldsymbol{\varepsilon}\cdot\mathbf{r})_{nj}(\boldsymbol{\varepsilon}^*\cdot\mathbf{r})_{jn}}{E_{nj}-\omega} = \frac{1}{\omega^2}\sum_j{}' \left[\frac{(\boldsymbol{\varepsilon}\cdot\mathbf{P})_{nj}(\boldsymbol{\varepsilon}^*\cdot\mathbf{P})_{jn}}{E_{nj}-\omega} - (E_{nj}+\omega)(\boldsymbol{\varepsilon}\cdot\mathbf{r})_{nj}(\boldsymbol{\varepsilon}^*\cdot\mathbf{r})_{jn} \right] \tag{3.8b}$$

for the absorption and the emission terms, respectively. In Eqs. (3.8) the quantities $\sum_j E_{ji}|\boldsymbol{\varepsilon}\cdot\mathbf{r}|_{ij}^2$ and $\sum_j |\boldsymbol{\varepsilon}\cdot\mathbf{r}|_{ij}^2$, $(E_{ij}=E_i-E_j)$ can be easily calculated by using well-known sum rules.[24] These relations are very useful for checking the connection between absorption-emission (emission-absorption) terms in the two gauges.

Computations have been done in the two gauges by resorting to two different methods. For Eq. (3.4) we have used the technique of differential equations,[25] while the expression of Eq. (3.7) has been calculated from direct summation and quadrature. By this method we have tested the accuracy of our calculations as well as the equivalence of the results concerning the absorption (emission) term [Eq. (3.8)] obtained in the two gauges.

The results shown in Tables I and II concern calculations done for linearly polarized light at 1060 and 530 nm, respectively. The values of the "absorption-emission" and "emission-absorption" terms are given explicitly for the magnetic quantum number $m=0$. They are expressed in atomic units and are divided by the intensity in W/cm^2. The values of the widths are reported in the sixth column. The shifts are obtained in the length gauge by summing the absorption-emission L_a and the emission-absorption L_e contributions. Within the velocity gauge V_a and V_e represent the same quantities, respectively, but one must add V_e+V_a to the contribution of the quadratic part of the Hamiltonian $1/I_0\omega^2$, which is equal to 3.815×10^{-15} cm^2/W at 1060 nm and 9.682×10^{-16} cm^2/W at $\lambda=530$ nm. The results presented in column 9 of the Tables I and II are the contributions from the $\mathbf{A}\cdot\mathbf{P}$ term of the Hamiltonian of Eq. (3.6). One sees that they become smaller and smaller as one approaches the theoretical continuum limit. Accordingly, the contribution of the A^2 term [$(\alpha^2/2)A^2 \rightarrow I/I_0\omega^2$ in a.u.], which is nearly compensated for by that coming from the $\mathbf{A}\cdot\mathbf{P}$ term for the ground state, prevails for highly excited states. It is responsible for a contribution to the level shift which is the same for all the levels of the spectrum (discrete and continuum). In contrast to the A^2 term, the $\mathbf{A}\cdot\mathbf{P}$ term provides complex values for the shift operator which can be calculated up to an arbitrary

TABLE I. Comparison between the contributions to second-order matrix elements of the rate $(\Delta^{(2)}-i\Gamma^{(2)})=(\Delta_{nl}-i\Gamma_{nl})/I$ computed in the length and in the velocity gauge. L_a is the contribution of the absorption-emission term and L_e is that of the emission-absorption term in the length gauge. V_a and V_e represent the same quantities expressed in the velocity gauge, respectively. Notice that $\Delta-i\Gamma=(1/I_0\omega^2+V_a+V_e)$. All the values are given in a.u. cm^2/W up to a factor of 10^{-16}. The calculations have been done for atomic levels with quantum numbers $n,l,m=0$ and for a linearly polarized light at 1060 nm. Only the L_a (V_a) terms contribute to the widths.

n	l	L_a	L_e	$\Delta^{(2)}$	$\Gamma^{(2)}$	V_a	V_e	V_a+V_e
1	0	−0.179	−0.144	−0.324	0	−21.09	−17.75	−38.84
2	0	4.73	−17.66	−12.93	0	−37.70	−13.74	−51.44
	1	4.22	−19.74	−23.96	0	−53.29	−9.17	−62.46
3	0	157.38	−102.82	54.55	0	23.86	−7.81	16.05
	1	249.38	−149.13	100.24	0	51.27	10.46	61.73
	2	204.76	−62.15	142.61	0	76.21	27.89	104.10
4	0	385.25	−347.63	37.62	12.456	8.22	−9.11	−0.89
	1	635.48	−594.97	40.51	16.184	19.87	−17.92	1.95
	2	483.66	−411.17	42.49	12.021	27.06	−23.13	3.93
	3	355.41	−328.75	26.66	4.77	31.35	−43.22	−11.87
5	0	895.72	−858.46	37.26	6.617	6.87	−8.13	−1.26
	1	1524.71	−1492.47	32.24	8.221	14.72	−21.01	−6.29
	2	1207.93	−1177.72	30.21	5.746	17.38	−25.70	−8.31
	3	990.83	−966.78	24.05	2.616	19.16	−33.63	−14.47
	4	730.23	−692.72	37.51	0.53	18.86	−19.86	−1.00
6	0	1823.33	−1789.96	33.50	3.904	5.28	−10.43	−5.15
7	0	3351.08	−3310.62	40.46	2.487	4.23	−2.28	1.94
8	0	5694.00	−5654.82	39.18	1.678	3.43	−2.76	0.66
9	0	9100.49	−9061.63	38.86	1.184	2.82	−2.47	0.35
10	0			38.7310	0.866	2.36	−2.14	0.22
20	0			38.5308	0.109	0.6671	−0.6492	0.0179
30	0			38.5177	0.0325	0.3069	−0.3021	0.0048
40	0			38.5148	0.0137	0.1749	−0.1729	0.002
Limit				38.5128	0			

TABLE II. Same as Table I except that the radiation wavelength is 530 nm.

n	l	L_a	L_e	$\Delta^{(2)}$	$\Gamma^{(2)}$	V_a	V_e	V_a+V_e
1	0	−0.202	−0.133	−0.335	0	−5.84	−4.11	−9.96
2	0	13.66	−9.50	4.16	0	−2.74	−2.72	−5.46
	1	24.42	−10.95	13.46	0	4.70	−0.86	3.84
3	0	63.98	−54.87	9.11	3.275	2.01	−2.53	−0.52
	1	99.55	−95.13	4.42	3.602	5.27	−10.49	−5.22
	2	66.36	−68.97	−2.61	1.620	6.87	−19.11	−12.24
4	0	185.23	−174.85	10.38	1.422	1.52	−0.78	0.74
	1	306.25	−289.60	16.65	1.447	3.29	3.74	7.03
	2	227.14	−208.16	18.98	0.665	3.68	5.66	9.34
	3	160.88	−151.56	9.32	0.132	3.68	−3.99	−0.31
5	0	440.71	−430.85	9.85	0.737	1.10	−0.87	0.23
	1	752.40	−741.25	11.15	0.729	2.23	−0.71	1.52
	2	592.79	−581.51	11.27	0.335	2.33	−0.69	1.64
	3	483.35	−473.91	9.43	0.085	2.34	−2.53	−0.19
	4	353.15	−343.58	9.57	0.009	2.28	−2.33	−0.05
6	0	905.05	−895.28	9.75	0.429	0.84	−0.70	0.14
7	0	1669.25	−1659.54	9.71	0.271	0.64	−0.55	0.087
8	0	2840.98	−2831.29	9.69	0.182	0.50	−0.44	0.057
9	0	4544.43	−4534.76	9.67	0.128	0.40	−0.36	0.040
10	0			9.65731	0.094	0.33	−0.30	0.03
20	0			9.63178	0.0117	0.0878	−0.0843	0.0035
30	0			9.62926	0.0034	0.0397	−0.0387	0.001
40	0			9.62865	0.0015	0.0224	−0.0220	0.0004
Limit				9.62821	0			

order. From the true level energies, one obtains the energy of any transition as well as the ionization limit by subtraction.

From the results of Tables I and II one may be tempted to consider A^2 as being the term responsible of the shift of the ionization limit. The confusion comes from the fact that in hydrogen and rare gases, the second-order $\mathbf{A}\cdot\mathbf{P}$ terms for the ground state, quasiexactly balance the effect of the A^2 term. This may not be a general rule. It will be shown in Sec. IV what care must be taken in predicting the behavior of the shifts of highly excited level at high intensity, on the grounds of second-order theory, by testing the convergence of the series (2.4).

IV. FOURTH-ORDER ENERGY SHIFTS

As a prelude to a more general calculation including all higher-order contributions, we consider the fourth-order corrections to the level shifts. The processes involved are represented, in the energy scale, by the six diagrams of Fig. 1(b). The shift of the level (n,l) calculated up to fourth order is

$$R_{n,n}=R_{n,n}^{(2)}+R_{n,n}^{(4)} , \tag{4.1}$$

where $R_{n,n}^{(2)}$ is given by Eqs. (3.2) or (3.6). The expression of $R_{n,n}^{(4)}$ in the length gauge is

$$R_{n,n}^{(4)}=\left[\frac{I}{I_0}\right]^2 \sum_{i,j,k\neq n}{}' \left[\frac{d_{ni}^{\pm}d_{ij}^{\pm}d_{jk}^{\mp}d_{kn}^{\mp}}{(E_{ni}\mp\omega)(E_{nj}\mp 2\omega)(E_{nk}\mp\omega)}+\frac{d_{ni}^{\pm}d_{ij}^{\mp}d_{jk}^{\pm}d_{kn}^{\pm}}{(E_{ni}\mp\omega)E_{nj}(E_{nk}\mp\omega)}+\frac{d_{ni}^{\mp}d_{ij}^{\pm}d_{jk}^{\mp}d_{kn}^{\pm}}{(E_{ni}\pm\omega)E_{nj}(E_{nk}\pm\omega)}\right] \tag{4.2a}$$

with

$$d^{+}\equiv D , \tag{4.2b}$$

$$d^{-}\equiv D^{*} . \tag{4.2c}$$

In Eq. (4.2a) the sum is to be taken over the upper and the lower signs. We note that the state $|n\rangle$ is excluded from the sums over intermediate states because of the presence of the projector Q in the expression of the shift operator $R(z)$. The matrix elements are calculated by using the method of coupled differential equations which needs not be repeated here.[25] The great interest of this method is that high-order matrix elements are evaluated exactly without encountering divergences, even when one or several photons are absorbed above the ionization limit.[8] This is because the problem is solved within a fully complex calculation scheme.

The calculations have been done for circularly polarized light. The results obtained after averaging over the magnetic quantum number are shown in Table III. The values of $\Delta_{nl}^{(2)}$ and $\Delta_{nl}^{(4)}$ are given in atomic units (a.u.) up to a factor $10^{-16}I$ W/cm^2 and $10^{-27}I^2$ W^2/cm^4, respectively. As expected we see that the second-order shifts are independent of the light polarization for the S states. By averaging over the magnetic and the orbital quantum numbers we define

TABLE III. Second-order ($\bar{\Delta}^{(2)}, \bar{\Gamma}^{(2)}$) and fourth-order ($\bar{\Delta}^{4}, \bar{\Gamma}^{4}$) contributions to the average shifts and widths of levels with quantum numbers n and 1. Notice that $\bar{\Delta}^{(k)}-i\bar{\Gamma}^{(k)}=[1/(2l+1)]\sum_{m=-l}^{l}[(\Delta^{(k)}-i\Gamma^{(k)})_{nlm}]/I^{k/2}$. The values are given for circularly polarized light at two different wavelengths (a) 530 nm for $\bar{\Delta}_a-i\bar{\Gamma}_a$ and (b) 1060 nm for $\bar{\Delta}_b-i\bar{\Gamma}_b$. The results are expressed in a.u. $\mathrm{cm}^k/\mathrm{W}^{k/2}$ up to a factor of 10^{-16} and 10^{-27} for second order and fourth order, respectively.

n	0	$\bar{\Delta}_a^{(2)}$	$\bar{\Gamma}_a^{(2)}$	$\bar{\Delta}_a^{(4)}$	$\bar{\Gamma}_a^{(4)}$	$\bar{\Delta}_b^{(2)}$	$\bar{\Gamma}_b^{(2)}$	$\bar{\Delta}_b^{(4)}$	$\bar{\Gamma}_b^{(4)}$
1	0	−0.335	0	-0.88×10^{-5}	0	−0.324	0	-0.74×10^{-5}	0
2	0	4.16	0	1.893	0.023	−12.93	0	−0.428	0
	1	10.89	0	2.099	0.018	−19.48	0	−1.166	0
3	0	9.11	3.27	0.217	0.0011	54.55	0	816.5	0.084
	1	8.72	2.77	0.147	0.0016	73.10	0	731.1	0.042
	2	4.27	1.24	0.080	0.0025	104.70	0	573.2	0.010
4	0	10.38	1.42	0.616	0.0032	37.62	12.45	10.79	0.086
	1	12.34	1.09	0.543	0.0032	41.03	12.19	9.71	0.038
	2	14.59	0.51	0.377	0.0005	43.22	9.19	7.0	0.048
	3	9.61	0.10	0.301	0.0002	34.19	3.57	6.01	0.086
5	0	9.85	0.74	1.469	0.0025	37.26	6.62	23.80	0.085
	1	10.33	0.54	1.394	0.0022	37.46	6.11	22.28	0.132
	2	10.59	0.25	1.248	0.0011	35.70	4.37	19.78	0.118
	3	9.60	0.06	0.925	0.00008	31.53	1.95	15.3	0.005
	4	9.63	0.006	0.669	0.00004	38.53	0.39	10.86	0.013
6	0	9.75	0.43	3.026	0.0018	33.53	3.90	44.82	0.096
	1	9.96	0.31	2.923	0.0015	28.96	3.50	38.88	0.113
	2	10.03	0.12	2.723	0.0007	20.58	2.44	32.46	0.081
	3	9.61	0.05	2.419	0.0006	16.67	1.15	34.90	0.034
	4	9.64	0.01	1.874	0.0023	38.43	0.31	28.23	0.004
	5	9.63	0.001	1.260	0.0002	38.54	0.035	20.91	0.002
10	0	9.66	0.094	23.16	0.0490	38.73	0.866	373.32	0.656

$$\Delta_n=\frac{1}{n^2}\sum_{l=0}^{n-1}\sum_{m=-l}^{+l}\Delta_{nlm}\ . \tag{4.3}$$

From these averaged values of the shifts, we determine the intensities at which $\Delta_n^{(2)}=\Delta_n^{(4)}$. These threshold intensities $I_{\mathrm{th}}(n)$ are shown in Table IV and are plotted in Fig. 2. Let us consider the curve representing the threshold intensity for the shift at $\lambda=530$ nm. We note that $I_{\mathrm{th}}(1)$ is very high ($>3\times10^{15}$ W/cm^2) for the ground state. This value is of the same order of magnitude as that calculated by other authors.[12,19] This means that a second-order calculation of the shift is relevant up to intensity values of few 10^{15} W/cm^2. Recently, corrections to the ground-state energy have been calculated up to tenth order.[20] These high-order contributions reinforce the effect of the fourth-order term so that $I_{\mathrm{th}}(1)$ is reduced by two orders of magnitude (about 10^{13} W/cm^2). For $n=2$, $I_{th}(2)$ falls down rapidly and exhibits an accidental minimum due to a near-resonant coupling, i.e., the energy gap between the $n=2$ and 4 levels approaches the one-photon energy. For $n>3$, the threshold intensities decrease monotonically with increasing n. The values of $I_{\mathrm{th}}(10)$ are less than 10^{11} W/cm^2, a value which is about two orders of magnitude lower than those involved in ATI experiments.[17,18]

TABLE IV. Threshold intensities $I_{\mathrm{th}}(n)$ in W/cm^2 corresponding to $\Delta_n^{(2)}=\Delta_n^{(4)}$, calculated for different values of the principal quantum number n. The results correspond to circularly polarized light whose wavelength is 530, 1060, and 10 600 nm. The numbers in square brackets are powers of ten.

n	$I_{\mathrm{th}}(n)$ $\lambda=530$ nm	$\lambda=1060$ nm	$\lambda=10\,600$ nm
1	3.8[15]	4.4[15]	5.6[11]
2	4.5[11]	1.82[12]	7.2[9]
3	5.33[12]	1.3[10]	7.0[8]
4	3.01[12]	5.25[11]	1.8[10]
5	1.01[12]	2.27[11]	1.0[9]
6	4.8[11]	1.05[11]	1.8[8]
10	4.10[10]	1.05[10]	

The same behavior is observed at 1060 and 10 600 nm. For the former wavelength the dip comes from the states $n=2$ and 3 whose energies differ approximately by that of one photon. The curves of Fig. 2 clearly show that the values of $I_{\mathrm{th}}(n)$ decrease with the photon energy. On the grounds of a comparison involving second-order and fourth-order terms, it is clear that second-order theory becomes more and more questionable for higher and higher excited states. The values obtained for $I_{\mathrm{th}}(n)$ are of practical interest in indicating the range of intensities within which the lowest-order term of the perturbations theory can represent adequately the level shifts.

We can go further in the discussion by comparing the values of the complex shift obtained from the first three terms of the perturbation expansion with the "nonperturbative" results computed previously by Chu and Cooper[21] and later by Shakeshaft and Tang.[22] The calculation of the widths and the shifts of the ground-state energy of hydrogen is done for large photon energies ($0.2\le\omega\le0.6$ a.u.) in the case of linearly polarized light. Following the notation of Chu and Cooper, F is the rms field strength

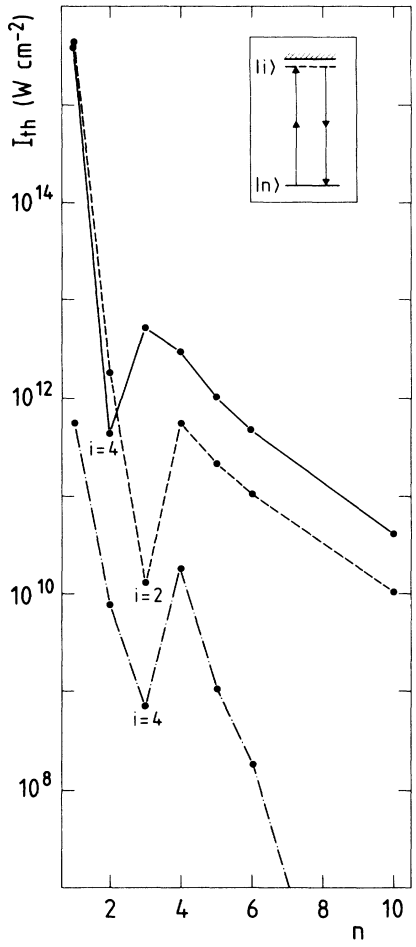

FIG. 2. Threshold intensity defined as being the intensity for which $\Delta_n^{(2)}=\Delta_n^{(4)}$, plotted as a function of the principal quantum number n. Solid line, dashed line, and dot-dashed line correspond to circularly polarized light at 530, 1060, and 10 600 nm, respectively. The dips observed on the curves come from a resonance induced in the fourth-order process by the state $|i\rangle$, illustrated in the inset.

expressed in a.u. ($0.01 \leq F \leq 0.1$ a.u. corresponds to $7\times10^{12} \leq I \leq 7\times10^{14}$ W/cm^2). In Table V we present the results given by the first nonvanishing term of the perturbation series (column 2), the sum of the first two terms (column 4), and that of the first three terms, (column 6). The disagreement, with respect to Chu and Cooper's values of the shift, is given in columns 3, 5, and 7. From these results several remarks can be made.

(a) The perturbation series appears to be well converging for values of F up to 0.05 a.u. ($I=1.7\times10^{14}$ W/cm^2).

(b) The convergence becomes better for increasing photon energies.

(c) For the intensity range under consideration, the first-order term of the perturbation series provides shifts in reasonable agreement with the more accurately computed results.[21,22]

(d) The threshold intensities corresponding to $\omega=0.2$, 0.3, and 0.6 a.u., are 5×10^{14}, 3×10^{14}, and 7×10^{15} W/cm^2, respectively. These values are within the same intensity range as that reported for the ground state in Table IV.

(e) The effects due to the interactions in the continuum spectrum can be observed through the width of the ground state. In the one-photon dominant ionization ($N_m=1$, $\omega=0.6$ a.u.) case many diagrams contribute to the width. Then we note that our results are in good agreement with the nonperturbative ones. But this agreement becomes poorer and poorer with the decrease of the number of contributing diagrams, i.e., in the $N_m=2$, $\omega=0.3$ a.u. and $N_m=3$, $\omega=0.2$ a.u. cases.

Summarizing the results presented in this section, the perturbation series for the shift operator appears to be less and less convergent as the principal quantum number increases, while, for the ground-state energy, this convergence gets better for increasing photon energies. However, the first terms of the $R^{\rm diag}(E)$ expansion are not sufficient to determine the true radius of convergence of the perturbation series. Only an all-order calculation can provide the right values of the level shifts.

V. SECOND-ORDER SHIFT OPERATOR IN THE CONTINUUM SPECTRUM

In Sec. II we emphasized the role played by the complex shift of atomic levels in the expressions of ATI probabilities. In particular, this last process requires a careful computation of diagonal matrix elements $R_{\alpha E,\alpha E}(E)$. To second order in the length gauge we have

$$R^{(2)}_{\alpha E,\alpha E}=\frac{I}{I_0}\sum_j{}'\left[\frac{D^*_{\alpha E,j}D_{j,\alpha E}}{E-E_j+\omega}+\frac{D_{\alpha E,j}D^*_{j,\alpha E}}{E-E_j-\omega}\right], \quad (5.1)$$

where $D_{\alpha E,j}=\langle\alpha E|\boldsymbol{\varepsilon}\cdot\mathbf{r}|j\rangle$, $|\alpha E\rangle$ is written for the continuum state of energy E, all other quantities have been already defined. The sum over j runs over the whole spectrum of the atom and thus the expression of $R^{(2)}_{\alpha E,\alpha E}$ contains continuum-continuum matrix elements such as $D_{\alpha E,\alpha' E'}$ which diverge when $E=E'$. This divergence is typical of multiphoton theory which requires the knowledge of dipole matrix elements between Coulomb states of well-defined orbital quantum numbers.[26] Thus the problem cannot be solved by the methods used to investigate the free-free transitions.[27] To find the origin of such a divergence we resort to the following well-known relations among momentum and position operators:[24]

$$\begin{aligned}\langle\alpha' E'|[\mathbf{P},H]_-|\alpha E\rangle&=-(E'-E)\mathbf{P}_{\alpha' E',\alpha E}\\&=-i(E'-E)^2\mathbf{r}_{\alpha' E',\alpha E}\ ,\end{aligned} \quad (5.2)$$

where use has been made of the relation

$$i(E'-E)\mathbf{r}_{\alpha' E',\alpha E}=\mathbf{P}_{\alpha' E',\alpha E}\ . \quad (5.3)$$

On the other hand, since $[\mathbf{P},H]_-=[\mathbf{P},1/r]_-$, one has

$$\begin{aligned}\langle\alpha' E'|[\mathbf{P},H]_-|\alpha E\rangle&=-i\langle\alpha' E'|\nabla(1/r)|\alpha E\rangle\\&=-i\left[\frac{\mathbf{r}}{r^3}\right]_{\alpha' E',\alpha E}\ .\end{aligned} \quad (5.4)$$

Let us define the function

TABLE V. Values of the complex shift $\Delta - i\Gamma$ in a.u. in the ground-state energy of hydrogen for various energies ω and field amplitude F ($F = I/7.019\times10^{16}$, where F is in a.u. and I in W/cm^2). The results at the second, fourth, and sixth order of the perturbation theory are given in columns 2, 4, and 6, respectively. Estimates of the disagreement between the values of Chu and Cooper (Ref. 21) and our present results are reported in columns 3, 5, and 7 (rate percent %). Numbers in square brackets are powers of 10.

F	$E_0+\Delta^{(2)}-i\Gamma^{(2)}$	Disagreement with Ref. 21 (%)	$E_0+(\Delta^{(2)}+\Delta^{(4)})-i(\Gamma^{(2)}+\Gamma^{(4)})$	Disagreement with Ref. 21 (%)	$E_0+(\Delta^{(2)}+\Delta^{(4)}+\Delta^{(6)})-i(\Gamma^{(2)}+\Gamma^{(4)}+\Gamma^{(6)})$	Disagreement with Ref. 21 (%)
			$\omega=0.2$ a.u.			
0.01	(−0.500 297, i0)	8[−6]	(−0.500 293, i0)	5[−6]	(−0.500 293, i0.9996[−7]	9[−5]
0.025	(−0.501 857, i0)	5[−2]	(−0.501 705, i0)	2.4[−2]	(−0.501 596, i0.2440[−4])	2[−3]
0.05	(−0.507 427, i0)	0.3	(−0.505 005, i0)	0.75	(−0.498 027, i0.1562[−2])	2
0.075	(−0.516 711, i0)	0.4	(−0.504 448, i0)	2.8	(−0.424 965, i0.1779[−1])	18
0.01	(−0.529 708, i0)	0.9	(−0.490 950, i0)	6		
			$\omega=0.3$ a.u.			
0.01	(−0.500 528, i0)	2[−3]	(−0.500 515, i0.3864[−5])	3[−4]	(−0.500 515, i0.3796[−5])	2[−4]
0.025	(−0.503 301, i0)	8[−2]	(−0.502 785, i0.1509[−3])	2[−2]	(−0.502 893, i0.1342[−3])	1[−3]
0.05	(−0.513 204, i0)	9[−1]	(−0.504 953, i0.2415[−2])	7[−1]	(−0.511 880, i0.1340[−2])	6[−1]
0.075	(−0.529 711, i0)	3	(−0.487 938, i0.1223[−1])	5	(−0.566 848, i0)	10
0.1	(−0.552 819, i0)	7	(−0.420 795, i0.3864[−1])	18		
			$\omega=0.6$ a.u.			
0.01	(−0.499 835, i0.1252[−3])	2[−6]	(−0.499 835, i0.1253[−3])	3[−5]	(−0.499 835, i0.1253[−3])	2[−5]
0.025	(−0.498 969, i0.7828[−3])	5[−4]	(−0.498 962, i0.7865[−3])	8[−4]	(−0.498 962, i0.7865[−3])	1[−3]
0.05	(−0.495 878, i0.3131[−2])	7[−3]	(−0.495 772, i0.3191[−2])	1.4[−2]	(−0.495 768, i0.3190[−2])	1.5[−2]
0.075	(−0.490 725, i0.7045[−2])	3[−2]	(−0.490 189, i0.7347[−2])	7[−2]	(−0.490 149, i0.7339[−2])	8[−2]

$$\rho_{\alpha' E',\alpha E} = \left[\frac{\boldsymbol{\varepsilon}\cdot\mathbf{r}}{r^3}\right]_{\alpha' E',\alpha E} . \tag{5.5}$$

By identifying Eqs. (3.13) and (3.15), one finds that

$$(\boldsymbol{\varepsilon}\cdot\mathbf{r})_{\alpha' E',\alpha E} = \frac{1}{(E'-E)^2}\rho_{\alpha' E',\alpha E} . \tag{5.6}$$

The matrix elements of the operator ρ thus defined are not divergent. They only require accurate calculations to warrant a good stability of the results. Equation (5.6) shows the reason why the matrix elements of $\boldsymbol{\varepsilon}\cdot\mathbf{r}$ diverge when $E'=E$: there exists a second-order pole which does not appear explicitly. By replacing the matrix element $(\boldsymbol{\varepsilon}\cdot\mathbf{r})_{\alpha' E',\alpha E}$ as given by Eq. (5.6) into Eq. (5.1), a fourth-order pole appears in the integral running over the energies of the continumm.

We have

$$R_{\alpha E,\alpha E} = \frac{I}{I_0}\sum_j{}' \left[\frac{\rho^*_{\alpha E,j}\rho_{j,\alpha E}}{(E-E_j)^4(E-E_j+\omega)} + \frac{\rho_{\alpha E,j}\rho^*_{j,\alpha E}}{(E-E_j)^4(E-E_j-\omega)}\right] . \tag{5.7}$$

The evaluation of the integrals in Eq. (5.7) requires both an analytical continuation of the functions $\rho_{\alpha E,j}$ onto the complex plane and the calculation of the successive derivatives of $|\rho_{\alpha E,j}|^2$. Such difficulties preclude any computation of $R^{(2)}_{\alpha E,\alpha E}$ in the form displayed in Eq. (5.7). The problem of handling high-order poles is encountered in both length and velocity gauges, but fortunately it is more easily solved in the latter. In the following lines a method is presented which avoids high-order poles. To this end we express the matrix element $R^{(2)}_{\alpha E,\alpha E}$ in the velocity gauge as

$$R^{(2)}_{\alpha E,\alpha E} = \frac{I}{I_0\omega^2}\left[\boldsymbol{\varepsilon}^*\cdot\boldsymbol{\varepsilon} + \sum_j{}' \left[\frac{\bar{Q}_{\alpha E,j}Q_{j,\alpha E}}{E-E_j+\omega} + \frac{Q_{\alpha E,j}\bar{Q}_{j,\alpha E}}{E-E_j-\omega}\right]\right] , \tag{5.8}$$

where

$$Q_{\alpha E,j} = \langle \alpha E|\boldsymbol{\varepsilon}\cdot\mathbf{P}|j\rangle , \tag{5.9a}$$

$$\bar{Q}_{\alpha E,j} = \langle \alpha E|\boldsymbol{\varepsilon}^*\cdot\mathbf{P}|j\rangle . \tag{5.9b}$$

Owing to the relations

$$(E-E_j)Q_{\alpha E,j} = i\rho_{\alpha E,j} , \tag{5.10a}$$

$$(E-E_j)\bar{Q}_{\alpha E,j} = i\rho^*_{\alpha E,j} , \tag{5.10b}$$

which are readily obtained from Eqs. (5.2) and (5.6), one finds

$$R^{(2)}_{\alpha E,\alpha E} = \frac{I}{I_0\omega^2}\left[\boldsymbol{\varepsilon}^*\cdot\boldsymbol{\varepsilon} - \sum_j{}' \left[\frac{\rho^*_{\alpha E,j}\rho_{j,\alpha E}}{(E-E_j+\omega)(E-E_j)^2} + \frac{\rho_{\alpha E,j}\rho^*_{j,\alpha E}}{(E-E_j-\omega)(E-E_j)^2}\right]\right] . \tag{5.11}$$

As a consequence of the commutation relations between the components of the momentum operator, $\bar{Q}$ and Q commute with each other, i.e., $[Q,\bar{Q}]_-=0$. Therefore we can add to the terms in the bracket of the right-hand side of Eq. (5.11), the vanishing quantity

$$\frac{1}{\omega}\langle \alpha E|[Q,\bar{Q}]_-|\alpha E\rangle=\frac{1}{\omega}\sum_j{}'(Q_{\alpha E,j}\bar{Q}_{j,\alpha E}-\bar{Q}_{\alpha E,j}Q_{j,\alpha E}) . \tag{5.12}$$

Then, by replacing the matrix elements of Q and $\bar{Q}$ by those of ρ according to Eqs. (5.10), one obtains, after a little algebra,

$$R^{(2)}_{\alpha E,\alpha E}=\frac{I}{I_0\omega^2}\left[\boldsymbol{\varepsilon}^*\cdot\boldsymbol{\varepsilon}+\frac{1}{\omega}\sum_j{}'\left[\frac{\rho^*_{\alpha E,j}\rho_{j,\alpha E}}{(E-E_j+\omega)(E-E_j)}-\frac{\rho_{\alpha E,j}\rho^*_{j,\alpha E}}{(E-E_j-\omega)(E-E_j)}\right]\right] , \tag{5.13}$$

or, equivalently,

$$R^{(2)}_{\alpha E,\alpha E}=\frac{I}{I_0\omega^2}\left\{\boldsymbol{\varepsilon}^*\cdot\boldsymbol{\varepsilon}+\frac{1}{\omega^2}\sum_j{}'\left[\left[\frac{1}{E-E_j}-\frac{1}{E+\omega-E_j}\right]\rho^*_{\alpha E,j}\rho_{j,\alpha E}+\left[\frac{1}{E-E_j}-\frac{1}{E-\omega-E_j}\right]\rho_{\alpha E,j}\rho^*_{j,\alpha E}\right]\right\} . \tag{5.14}$$

The contribution coming from the sum over the discrete spectrum $\sum_j B_{\alpha E,j}$ may be extracted from the generalized sum $\sum_j'$ and computed easily. The remaining terms, which give the continuum spectrum contribution, are evaluated from integrals involving the three simple poles $E_p=E_j$ and $E_p=E_j\pm\omega$ (throughout the paper E_p will be written for the energy of the pole). Our method leads to a considerable simplification and enables one to put $R^{(2)}_{\alpha E,\alpha E}$ into a fully calculable form. It avoids the difficulties coming from the fourth-order poles and the second-order poles implicitly contained in the expressions of Eqs. (5.7) and (5.8), respectively.

Practically, the expression of $\rho_{\alpha E,\alpha' E'}$ [Eq. (5.5)] involves a complicated integral over the coordinate r which is evaluated by resorting to generalized hypergeometric functions.[28,29] We note that the numerical technique must take care of problems arising from the slow convergence of the series within particular energy domains.

We are faced with the problem of calculating integrals of the form

$$I_{\alpha\alpha'}(E,E_p)=\int_0^\infty dE'\frac{f_{\alpha\alpha'}(E,E')}{E_p-E'} , \tag{5.15}$$

appearing on the right-hand side of Eq. (5.14) [$f_{\alpha\alpha'}(E,E')\equiv|\rho_{\alpha E,\alpha' E'}|^2$]. When $E_p<0$, $I_{\alpha\alpha'}(E,E_p)$ is obtained by usual quadrature. For positive values of E_p, resonance poles appear which make it necessary to resort to the following procedure. We introduce a Gaussian function in such a way that

$$I(E,E_p)=\int_0^\infty dE'\frac{f(E,E')-f(E,E_p)e^{-(E_p-E')^2}}{E_p-E'}+f(E,E_p)\int_0^\infty dE'\frac{e^{-(E_p-E')^2}}{E_p-E'} , \tag{5.16}$$

where for clarity the subscripts α and α' have been dropped; they will be easily restored when necessary. The first integral on the right-hand side of Eq. (5.16) is no longer singular and can be calculated by numerical quadrature. The integrand of the second integral is a simple analytic function which can be continued onto the complex plane. By choosing a suitable path of integration we find that

$$J(E_p)=\int_0^\infty dE'\frac{e^{-(E_p-E')^2}}{E_p-E'}=-\tfrac{1}{2}E_1(E_p^2)-i\pi . \tag{5.17}$$

The principal value of $J(E_p)$ is now expressed in terms of the exponential integral $E_1(E_p^2)$. By using the result of Eq. (5.17), we can write Eq. (5.16) in the form

$$I(E,E_p)=g(E,E_p)-i\pi f(E,E_p) , \tag{5.18}$$

where

$$g(E,E_p)=\int_0^\infty dE'\frac{f(E,E')-f(E,E_p)e^{-(E_p-E')^2}}{E_p-E'}-\tfrac{1}{2}f(E,E_p)E_1(E_p^2) . \tag{5.19}$$

At this stage of our discussion we have surmounted the major difficulties encountered in the calculation of the second-order element of the matrix representation of the level shift operator. However, by examining the expression of $g(E,E_p)$ in Eq. (5.19), we see that a problem still remains concerning the exponential integral which goes to infinity when $E_p\to 0$.

This complication arises in two circumstances.

(i) When $E\to 0$ and $E_p=E$, the quantity $f(E,E)E_1(E^2)$ of Eq. (5.19) can be accurately computed for $E>10^{-3}$. For smaller values, some difficulties of convergence affect the computation of the function $f(E,E')$. This region will not be explored in the present account.

(ii) When E approaches the energy of one photon ($E\to\omega$ and $E_p=E-\omega$), the integral $I(E,E_p)$ has a discontinuity at $E=\omega$. Over the energy range $(0,\omega)$, the integral $I(E,E-\omega)$, as given by Eq. (5.15), is real and can thus be evaluated by quadrature (Fig. 3). In contrast, for $E>\omega$, the resonant pole $E_p=E-\omega$ lying on the positive real axis makes the integral complex in the form shown in Eq. (5.18). Correlatively, the function $f(E,E-\omega)$ appearing in this equation no longer exists on the low-energy side of the discontinuity, while it takes

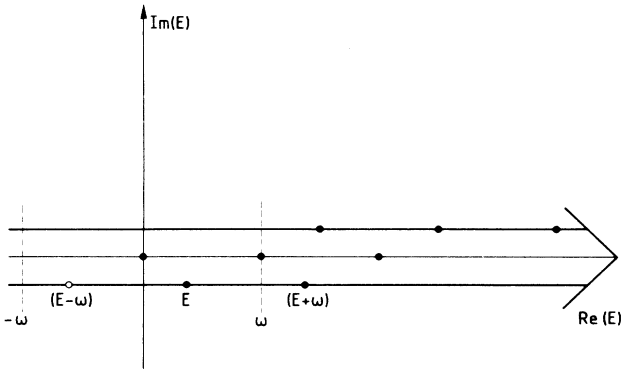

FIG. 3. Diagram indicating three different positions of the triplet pole which correspond to energies $E-\omega$, E, and $E+\omega$ lying on the real energy axis of the complex energy plane. The resonance poles of the integral $I(E,E_p)$ are marked by crosses. When energy decreases, the two poles $E-\omega$ and E move toward the origin of the energies they reach successively. For $0<E<\omega$, the lowest-energy pole vanishes. It is marked on the figure by an open circle. The vertical dashed line represents the discontinuity.

on the well-defined value $f(\omega,0)$ in the near vicinity of ω on the high-energy side. Furthermore, when $E-\omega\rightarrow 0+$ the term $f(E,E-\omega)E_1((E-\omega)^2)$ goes to infinity [$E_1(x)\rightarrow\infty$ when $x\rightarrow 0$]. The singularity coincides with the lower bound of the integral $I(E,E-\omega)$. Such a situation would not happen if we had calculated the contribution of the resonance pole for the true complex values of the energy. Nevertheless, we can compute the real part of the shift operator [Eq. (5.19)] for energy values as close as ω, which is necessary for our present discussion.

VI. RESULTS AND DISCUSSION

In this section we present the results concerning the diagonal matrix element calculations of the shift operator in the continuum spectrum. As we have seen in Sec. V, $R^{(2)}_{\alpha E,\alpha E}$ is a complex function which can be conveniently expressed in the form

$$R^{(2)}_{\alpha E,\alpha E}=\Delta_{\alpha E}-i\Gamma_{\alpha E}\ . \tag{6.1}$$

That $\Gamma_{\alpha E}$ goes to zero when the energy E goes to infinity is easily seen from Eqs. (5.14) and (5.18), which enable one to write $\Gamma_{\alpha E}$ as

$$\Gamma_{\alpha E}=\pi[f(E,E)-f(E,E+\omega)]+\pi[f(E,E)-f(E,E-\omega)]\ , \tag{6.2}$$

where the contributions of the three poles $E_p=E$ and $E_p=E\pm\omega$ appear explicitly. Since ω becomes negligible compared to E when $E\rightarrow\infty$, all the functions of Eq. (6.2) tend toward the same value and $\Gamma_{\alpha E}$ goes to zero. When $E<\omega$, we know (Sec. V and Fig. 3) that only two poles contribute in the calculation of $R^{(2)}_{\alpha E,\alpha E}$ ($E_p=0$ and $E_p=E+\omega$). We find that in this case $\Gamma_{\alpha E}$ decreases with E. The disappearance of the pole $E_p=E-\omega$ in this energy region produces a switchoff of the function $f(E,E-\omega)$ and thus induces a discontinuity in the behavior of $R^{(2)}_{\alpha E,\alpha E}$ at $E=\omega$. The effect of this discontinuity, which is very pronounced for low orbital states, becomes less and less sensitive as l increases. In Fig. 4 are the plots $\Gamma_{\alpha E}/I$ as a function of E/ω ($\lambda=1060$ nm). The energy in the continuum is expressed in units of the photon energy. For the orbital states depicted, the discontinuity still exists but is "smoothed" and gives rise to a maximum around $E/\omega=1$. This maximum, which is observed on all the curves, is more and more damped when one goes towards higher values of l.

The other quantity we report is the real part $\Delta_{\alpha E}$ of the shift operator in the continuum spectra. From Eqs. (5.14) and (5.19) we can write $\Delta_{\alpha E}$ in the form

$$\Delta_{\alpha E}=\frac{I}{I_0\omega^2}\left[1+\frac{1}{\omega^2}\left[\sum_j B_{\alpha E,j}+2g(E,0)-g(E,E+\omega)-g(E,E-\omega)\right]\right]\ , \tag{6.3}$$

which requires the calculation of the discrete spectrum contribution in addition to the evaluation of three integrals.

The results of the numerical calculations are shown in Fig. 5 ($\lambda=1060$ nm). The intensity-independent quantity $\Delta_{\alpha E}/I$ is plotted as a function of the energy for several values of the orbital quantum number l. We note that the shift $\Delta_{\alpha E}/I$ is a monotonic function over a very large en-

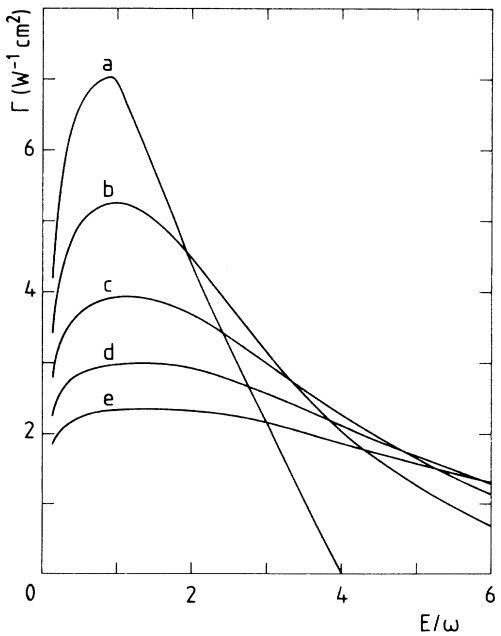

FIG. 4. Rate $\Gamma=10^{15}\,\Delta_{\alpha E}/I$ in a.u. cm^2/W giving the width as a function of the normalized energy E/ω for several values of the orbital quantum number l. (*a*) $l=8$, (*b*) $l=10$, (*c*) $l=12$, (*d*) $l=14$, and (*e*) $l=16$.

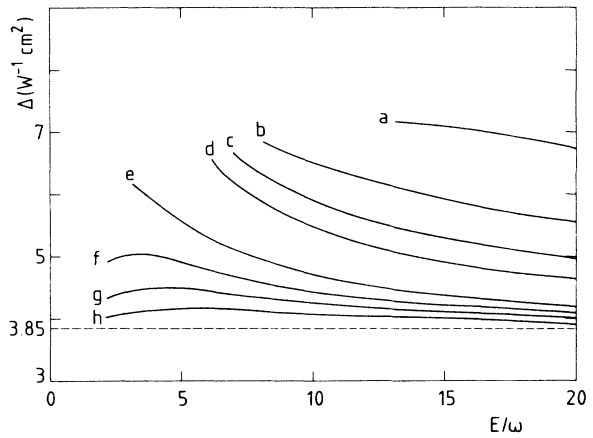

FIG. 5. Rate $\Delta = 10^{15}\ \Delta_{\alpha E}/I$ in a.u. cm^2/W representing the shift as a function of the normalized energy E/ω for several values of the orbital quantum number l. (*a*) $l=2$, (*b*) $l=3$, (*c*) $l=4$, (*d*) $l=5$, (*e*) $l=8$, (*f*) $l=10$, (*g*) $l=12$, and (*h*) $l=15$. The dashed line depicts the average quantity $1/I_0\omega^2$ ($I_0 = 1.4 \times 10^{17}$W/cm^2).

ergy range. It decreases and tends towards the value $1/I_0\omega^2$ [average value of the A^2 term of the Hamiltonian of Eq. (3.6)] as $E \to \infty$. Notice also that $\Delta_{\alpha E}$ becomes smaller and smaller with increasing l. $\Delta_{\alpha E}/I$ remains practically constant and equal to the average A^2 energy for $l > 10$. This result, which is general for all the curves, corroborates that obtained for highly excited discrete states. It shows that the whole spectrum is shifted upwards by an amount of energy equal to $I/I_0\omega^2$, while each state undergoes its own energy correction. On the low-energy side, we are faced with the discontinuity that has been encountered in the calculation $\Gamma_{\alpha E}$. This divergent behavior is due to a failure of the lowest-order perturbation theory within particular energy ranges. Its effect becomes unobservable for $l > 10$ because of the weakness of the matrix element $f(E, E-\omega)$.

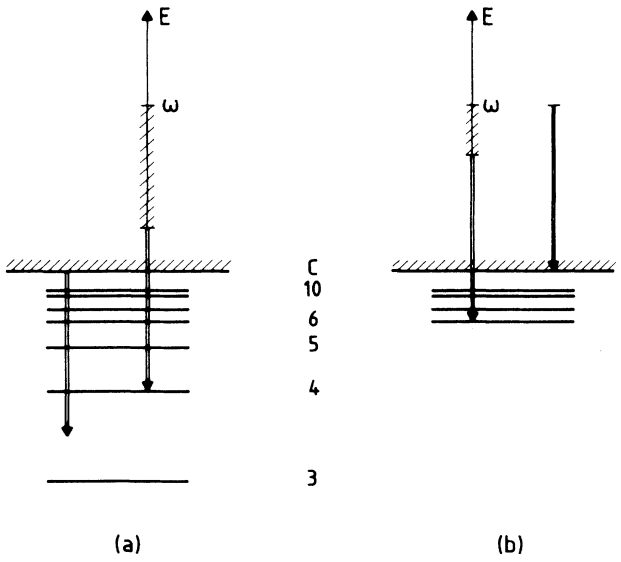

FIG. 6. Diagram representing the energy levels of atomic hydrogen belonging to the l channel. (a) $l=0,1,2$; (b) $l=5$. Each discrete level is labeled by its principal quantum number. The thick lines indicate the photon energy. The resonant state with the lowest energy $\bar{E}_{nl}$ is shown by an arrow. The shaded part of the energy axis is the region perturbed by the resonant discrete states. Its length decreases when l increases.

In calculating $\Delta_{\alpha E}$, an additional difficulty arises from the summation $\sum_j B_{\alpha E,j}$ over the discrete intermediate states included in the second-order matrix elements $R^{(2)}_{\alpha E,\alpha E}$ [Eq. (6.3)]. By varying E, the emission-absorption term gives rise to resonances induced successively by all the discrete states lying within the "dropping zone" $(\omega + \bar{E}_{nl}) \le E \le \omega$ of the emitted photon (Fig. 6). For the l channel, $\bar{E}_{nl}$ is defined as being the smallest resonant energy for which $\omega + \bar{E}_{nl}$ is both positive and minimum. Since $n \ge l+1$, $\bar{E}_{nl}$ increases with l and thus with n. This energy limit moves upwards in such a way that the resonant region becomes narrower and narrower.

As a last remark we want to emphasize the central role played by the complex shift in ATI. The transition amplitude given by Eq. (2.10) shows that $\Gamma_{\alpha E}$ acts in the denominator as well as in the exponentials as a damping term which is responsible of the width and the amplitude of the ATI peaks.

VII. CONCLUSIONS

We have presented the results of computations concerning the second-order shift operator with the intent of understanding its role in processes such as ATI. In addition to those dealing with the discrete spectrum, we have given some results for the continuum spectrum which were not known before. To make possible such calculations, new expressions for the continuum-continuum matrix elements of the second-order shift operator have been setup. More precisely, we have shown how the problems arising from the fourth-order poles in $R^{(2)}_{\alpha E,\alpha E}$ [Eq. (5.7)] could be solved.

Our calculation has put forward the drastic limitations of the second-order approximation for $R^{\rm diag}(E)$ with respect to the intensity. For the discrete spectrum the convergence of the $R^{\rm diag}$ expansion has been studied by comparing second-order to fourth-order terms. We have thus defined a threshold intensity $I_{\rm th}$ beyond which the shift is no longer correctly given by the second-order term of the perturbation series. This intensity has been found to decrease from 10^{15} to 10^{10} W/cm^2 when the principal quantum number increases from 1 to 10. From these values one can predict that the $R^{\rm diag}$ series will be quickly divergent with intensity for Rydberg states. Thus our results confirm that it is now of outmost importance to study how the $R^{\rm diag}(E)$ expansion behaves.

Concerning the computation in the continuum spectrum, we have been faced with two major difficulties: (i) that coming from the resonances induced by the discrete states within the energy range $(\bar{E}_{nl}+\omega, \omega)$ in the calculation of $\Delta_{\alpha E}$, and (ii) that coming from a resonance pole located at the origin of the real axis ($E_p = 0$) which pro-

duces a discontinuity for both $\Delta_{\alpha E}$ and $\Gamma_{\alpha E}$ at $E=\omega$. As shown in Sec. II this difficulty could be avoided in calculations involving $R^{\text{diag}}(z)$ instead of $R^{(2)}(E)$, i.e., in an all-order theory where the true complex energy is taken into account self-consistently. This problem will be discussed in a forthcoming account.

ACKNOWLEDGMENTS

The authors are grateful to Dr. C. Manus for useful conversations. They would like to thank Dr. V. B. Sheorey for his comments on the evaluation of radial integrals, and Dr. N. K. Rahman for many useful discussions.

[1]M. L. Goldberger and K. M. Watson, *Collision Theory* (Wiley, New York, 1964).

[2]L. Mower, Phys. Rev. **142**, 799 (1966).

[3]C. Cohen-Tannoudji, Cargese Lect. Phys. **2**, 347 (1967).

[4]M. Edwards, Liwen Pan, and L. Armstrong, Jr., J. Phys. B **17**, L515 (1984); **18**, 1927 (1985).

[5]Z. Bialynicka-Birula, Phys. Rev. A **28**, 836 (1983); J. Phys. B **17**, 3091 (1984).

[6]Z. Deng and J. H. Eberly, Phys. Rev. Lett. **53**, 1810 (1984); J. Opt. Soc. Am. **B2**, 486 (1985).

[7]P. Lambropoulos, Phys. Rev. A **9**, 1992 (1974).

[8]R. Shakeshaft, J. Opt. Soc. Am. **B4**, 705 (1987).

[9]Y. Gontier, N. K. Rahman, and M. Trahin, Phys. Rev. A **14**, 2109 (1976).

[10]M. Crance, in *Multiphoton Ionization of Atoms*, edited by S. L. Chin and P. Lambropoulos (Academic, New York, 1984), p. 65.

[11]A. Raczynski and J. Zaremba, J. Phys. B **19**, 3895 (1986).

[12]Numerous references concerning calculations of level shifts can be found in the paper of E. Arnous, J. Bastian, and A. Maquet, Phys. Rev. A **27**, 977 (1983). In this paper, second-order light shifts of discrete levels of hydrogen are calculated up to $n=5$ for linearly polarized light, while only the fourth-order shift of the ground state is reported. Our results concerning second-order corrections in linear polarization are in excellent agreement with the above-mentioned ones.

[13]Y. Gontier and M. Trahin, Phys. Rev. A **19**, 264 (1979).

[14]Y. Gontier, N. K. Rahman, and M. Trahin, Phys. Rev. A **37**, 4694 (1988).

[15]S. Libermann, J. Pinard, and A. Taleb, Phys. Rev. Lett. **50**, 888 (1983).

[16]L. Hollberg and J. L. Hall, Phys. Rev. Lett. **53**, 230 (1982).

[17]R. R. Freeman, P. H. Bucksbaum, H. Milchberg, S. Darrack, D. Schumacher, and M. E. Geusic, Phys. Rev. Lett. **59**, 1092 (1987).

[18]P. Agostini, A. Antonetti, P. Breger, M. Crance, A. Migus, H. G. Muller, and G. Petite (unpublished).

[19]L. Pan, B. Sudaram, and L. Armstrong, Jr., J. Opt. Soc. Am. B **4**, 754 (1987).

[20]L. Pan, K. T. Taylor, and C. W. Clark, Phys. Rev. Lett. **61**, 2673 (1988).

[21]S. Chu and J. Cooper, Phys. Rev. A **32**, 2769 (1985).

[22]R. Shakeshaft and X. Tang, Phys. Rev. A **36**, 3193 (1987).

[23]L. Rosenberg, Phys. Rev. A **18**, 2557 (1978).

[24]H. A. Bethe and E. E. Salpeter, *Quantum Mechanics of One- and Two-Electron Atoms* (Academic, New York, 1957).

[25]Y. Gontier and M. Trahin, Phys. Rev. **172**, 83 (1968); Phys. Rev. A **4**, 1896 (1971).

[26]Y. Gontier and M. Trahin, in *Atomic and Molecular Processes with Short Intense Laser Pulses*, edited by A. D. Bandrauk (Plenum, New York, 1988).

[27]M. Gavrila, A. Maquet, and V. Veniard, Phys. Rev. A **32**, 2537 (1985); **33**, 2826 (1985).

[28]W. Gordon, Ann. Phys. (Leipzig) **2**, 1031 (1929).

[29]K. Rzazewski and R. Gröbe, Phys. Rev. Lett. **54**, 1729 (1985).